Proceedings of ICRC 2001: 4007 © Copernicus Gesellschaft 2001

ICRC 2001

Leptons with E>200 MeV trapped in the earth's radiation belts

E. Fiandrini, G. Esposito, B. Bertucci, B. Alpat, R. Battiston, W. J. Burger, G. Lamanna, and P. Zuccon

University and INFN of Perugia

Abstract. Accurate measurements of electron and positron fluxes in the energy range 0.2−10 GeV have been performed with the Alpha Magnetic Spectometer (AMS) at altitudes of 370−390 km in the geographic latitude interval $\pm 51.7^{\circ}$. We describe the observed under-cutoff lepton fluxes outside the region of the South Atlantic Anomaly (SAA). The separation into *quasi-trapped*, long lifetime ($>$ 1 s), and *albedo*, short lifetime ($<$ 300 ms), components is explained in terms of the drift shell populations observed by the AMS. The flux distributions as a function of the canonical adiabatic variables L, α_o are presented for the interval $0.95 < L < 3$, $0^{\circ} < \alpha_o < 90^{\circ}$ for electrons (E<10 GeV), and positrons E(<3 GeV). The results are compared with existing data at lower energies. The properties of the observed under-cutoff particles are also investigated in terms of their residence times and geographical origin.

1 Introduction

Evidence for high energy (up to few hundreds of MeV) electrons and positrons trapped beneath the Inner Van Allen Belts has been published during last 20 years. At these energies, the existing data come from the measurements carried out by the Moscow Engineering Physics Institute. Data were taken with different instruments placed on satellites and the Mir station (Voronov, 1987),(Galper, 1986), (Akimov, 1987). These data proved the existence of ~ 100 MeV trapped leptons both in the Inner Van Allen Belts (*stably-trapped*) and in the region below (*quasi-trapped*), and determined their charge composition (Averin, 1988) and (Galper, 1997). The Russian measurements concern mainly the region of the SAA; very little data is available at the corresponding altitudes outside the SAA.

The ratio between e^+ and e^- is found to depend strongly on the position at which the observation is made. In the SAA, electrons dominate positrons by a factor ~ 10, a ratio similar to that observed for the cosmic fluxes, while outside the SAA the two fluxes are similar and comparable to the e^+ flux inside the SAA (Galper, 1986) [1].

In this contribution, we present the results of a study of the under-cutoff lepton fluxes in the ~ 1 GeV energy region based on the high statistic data sample of the AMS.

2 AMS and the STS-91 flight

The AMS is large acceptance ($\sim 0.16\,\mathrm{m^2 sr}$) device designed to operate on the International Space Station (ISS) for an observational period of three years. A prototype version of the detector, consisting of a high resolution silicon tracker providing an analyzing power of $\mathrm{BL}^2 = 0.14\,\mathrm{Tm}^2$ in the field of the permanent magnet, a plastic scintillator time-of-flight system, and a threshold aerogel Cerenkov counter for *ep* discrimination, was operated onboard the shuttle Discovery during a 10-day flight (STS-91) in June 1998. The shuttle Discovery orbited at geodesic altitudes between 370-390 km with an inclination of 51.7° in the GTOD reference frame. The details of the flight and first results have been presented at the previous ICRC in Salt Lake City (Becker, 1999).

The AMS Field-of-View (FoV) in the (L,α_0) coordinate space is fixed by the orbital parameters (geographic location and attitude) and the detector acceptance. The SAA region was excluded in this analysis. The resulting AMS FoV is compared in Fig. 1 to the coverages provided by satellite and balloon-borne detectors. The South Atlantic anomaly was excluded in this analysis.

3 Under-cutoff Lepton Fluxes

To reject the cosmic component of the measured lepton fluxes [2], the lepton trajectories in the earth's magnetic field were traced using a 4^{th} order Runge Kutta method with adaptive step-size. The equation of the motion was solved numerically and a particle was classified as trapped if its trajectory reached an altitude of 40 km, taken as the dense atmosphere limit, before its detection in AMS.

Correspondence to: E. Fiandrini
(emanuele.fiandrini@pg.infn.it)

[1] a second group reports a lower e^- excess ($\sim$ 2) for the SAA (Kurnosova, 1991)

[2] The details on the detector performances, lepton selection and background estimation can be found in (Alcaraz, 2000).

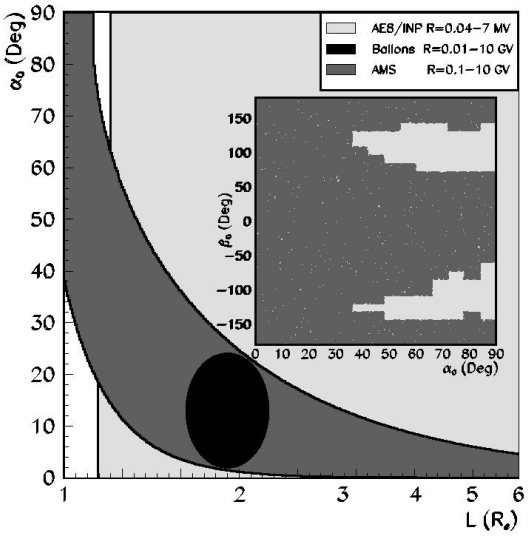

Fig. 1. Comparison among field of view of AMS, balloons and satellite data in (L,α_o). In the small plot, the AMS coverage in β_o vs α_o is shown.

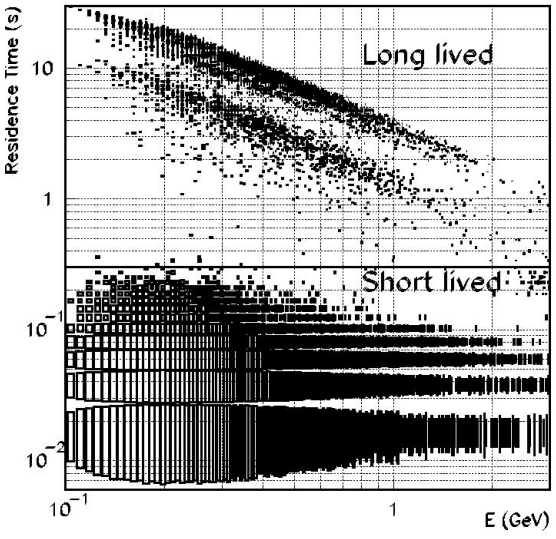

Fig. 2. Residence time vs energy for e^+. The same structure is observed for e^-

Although satisfactory in most cases, this approach is less stable when the particle rigidity falls in the penumbra region, close to the cutoff value. To treat the penumbra region, we defined an effective cutoff R_{eff} as the maximum rigidity value at a given magnetic latitude θ_m for which no traced lepton was found to be of cosmic origin. We rejected from our sample all particles with $R > R_{eff}$.

The residence, or flight times T_f, of the under-cutoff particles are computed, i.e. the total time spent by each particle above the atmosphere, before and after detection. The geographical location where the trajectories intercept the atmosphere determine the leptons' *production* and *impact* points.

The residence time distribution as a function of energy is shown in Fig. 2 for positrons; an identical behaviour is seen for electrons. The lepton residence times do not exceed $\sim$ 30 s, with 52% of e^- and 38% of e^+ having a $T_f < 0.3$ s independent of their energy, referred to as the *short-lived* populations in (Alcaraz, 2000). The corresponding impact/production points for the latter are spread over two bands on either side the magnetic equator. A scaling law, $T_f \approx E^{-2}$, is observed for the remaining leptons (the *long-lived* populations), which are localized in two distinct and limited regions[3] separated by a difference in T_f of $\geq$ 1s. The role of the two regions, i.e. zone of production/impact, is inverted depending on the charge of the leptons.

4 Interpretation with an Adiabatic Approach

The behaviour observed in the under-cutoff lepton data can be explained in terms of the geometry of the drift shells crossed by the AMS during the shuttle flight, and in particular by the fact that all the shells evolve partially in the atmosphere. Therefore for the population of particles detected, no permanent trapping can occur. The residence times are determined by the periodicity of the drifting (T_d) or bouncing ($T_b \ll T_d$) motion, and the fraction of the shell surface lying above the atmosphere.

The impact/production points correspond to the intersection of the shell surfaces with the atmosphere, where particles generated in interactions are injected into the shells. Long-lived and short-lived particles move along shells with different values of B_m or, equivalently α_0, which determine the mirror height on each field line. For high B_m values, or low α_0, the mirror height is very low and the shells penetrate into the atmosphere along all longitudes. The yellow bands in Fig. 4, which correspond to the shells with $\mathrm{B_m} \geq 0.48\,\mathrm{L}^{0.41}$ Gauss, are consistant with the extrapolated impact/production points of the AMS observed short-lived particles. When B_m is lower, or α_0 closer to 90°, the shells enter the atmosphere uniquely in the region of the SAA. The blue region in Fig. 4, which corresponds to shells with $\mathrm{B_m} \leq 0.48\,\mathrm{L}^{0.41}$ Gauss, is consistant with the extrapolated impact/production points of the observed long-lived component.

For the description of under cutoff fluxes, the energy E, the L-shell and the equatorial pitch angle α_0 were used. A three-dimensional grid (E, L, α_0) was defined to build flux maps; a linear binning in α_0 and logarithmic variable size for L and E bins were choosen to optimize statistics for each bin. Interval limits and bin widths are shown in Table 1.

The flux maps in (L, α_0) at constant E give the distribution of particle populations at the altitude of AMS. Nine maps at constant E have been made. Two different maps for two different energy bins for e^+ and e^- are shown in Fig. 4. The

[3] for the corresponding data distributions (*long* and *short*) refer to (Alcaraz, 2000)

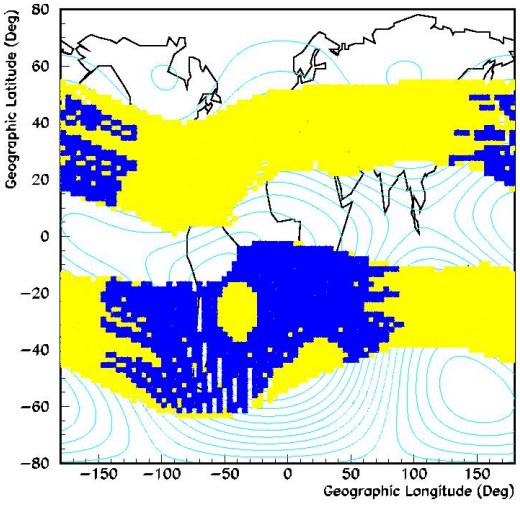

Fig. 3. Distribution of intersection points with atmosphere for the drift shells crossed by AMS. Yellow region corresponds to shells with $B_m \geq 0.48\,L^{0.41}$ G, blue one to $B_m \leq 0.48\,L^{0.41}$ G

flux is limited by the cutoff rigidity R_c: on a given shell only particles with R $\leq R_c$ are allowed to populate the shell, thus only low energy particles can populate higher shells.

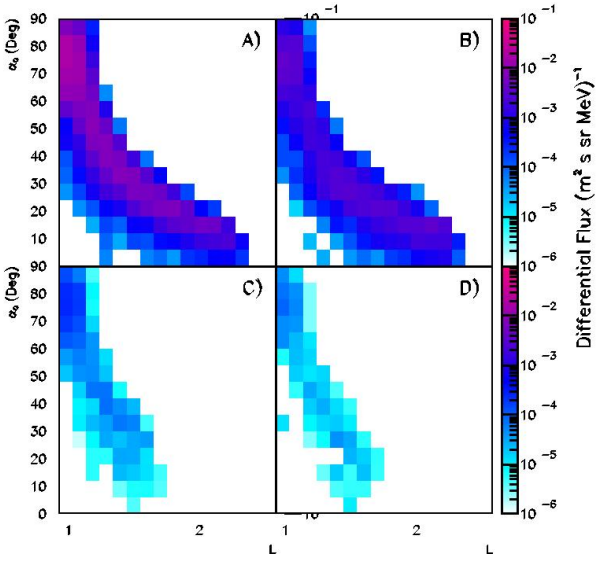

Fig. 4. Flux maps for 2 different energy bins: A), B) e^+, e^- between 0.315≤E≤0.486 GeV and C), D) e^+, e^- between 1.77≤E≤2.73 GeV

	N bin	Limit	Bin Width
E	9	0.205-10 GeV	0.187 (log.)
L	16	0.95-3	0.031 (log.)
α_0	15	$0^o - 90^o$	6^o (lin.)

Table 1. Bin limits used for AMS data binning

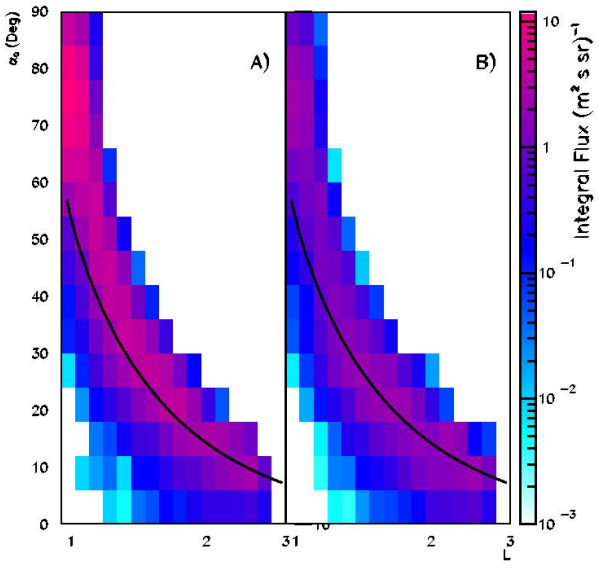

Fig. 5. Integral flux maps for e^+ (A) and e^- (B) between 0.205≤E≤2.73 GeV

The e^+, e^- flux maps and their ratio in the energy interval 0.2-2.7 GeV are shown in Figs. 5 and 6 respectively. In both plots, the solid line identifies the lower boundary in (L,α_o) for which no leptons can be found with residence times larger than 0.3 s. Above the curve, at higher values of α_o, the long-lived component of fluxes begins to dominate. This behaviour is illustrated in Fig. 7 where the same distributions, integrated over α_o (C,D) and L (A,B), are shown. The contributions of leptons with $T_f < 0.3$ s and $T_f > 0.3$ s are represented with dashed and solid lines respectively. Above $\alpha_o > 60^o$ the flux is substantially due to the long-lived component; the e^+ intensity represents $\approx 80\%$ of the total leptonic flux, while being at the same level or smaller than the e^- flux in the low α_o region. In L, the long-lived component dominates only at very low values where the positron excess is more pronounced.

This can be seen in the energy spectra for particles with $\alpha_0 \geq 70^o$, shown in Fig. 8, which is superimposed with measurements from MARIYA at lower energy (Galper, 1997). In the high pitch angle region the e^+ is higher than the e^- flux by a factor ~ 4.5, in contrast with MARYA data which indicate the same level of flux for both e^+ and e^-.

5 Conclusion

The AMS data indicates clearly the existence of leptonic radiation belts underneath the Inner Van Allen belts with particle energies of several GeV. The measured fluxes are not stably trapped since the corresponding drift shells are not closed over the SAA region.

At any given L, a critical value of the equatorial pitch angle, α_c, can be defined to distinguish the long, or *quasi-trapped*, and short-lived, or *albedo*, components of the fluxes. The same value is found to separate the regions where the

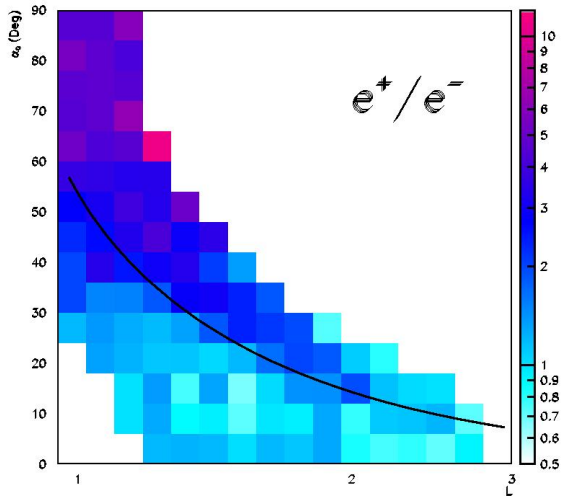

Fig. 6. Integral e^+/e^- ratio between 0.205≤E≤2.73 GeV

e^+/e^- ratio is above or around the unity: the charge composition shows a dominance of positively charged leptons in a definite region of the (L,α_o) space above $\alpha_c(L)$.

The interaction of primary cosmic rays and inner radiation belt protons with atmospheric nuclei in the regions of shell intersection with atmosphere are a natural mechanism of the production of secondary leptons through the $\pi - \mu - e$ or $\pi - \gamma - e$ decay chains. This naturally leads to a e^+ excess over e^- and seems suitable to explain the observed charge ratio for *quasi-trapped* flux (Voronov, 1995a). However, for the *albedo* flux the charge ratio is of the order of unity, as seen in Fig. 6, and other mechanisms might be present.

Acknowledgements. We gratefully acknowledge the contribution ofour collegues in AMS. We are also grateful to P.Lipari for useful discussions on the interpretation of AMS data. We greatly benefit of the software libraries (UNILIB,SPENVIS) developed in the context of the Trapped Radiation ENvironment Development (TREND) project for ESTEC, and we thank D.Heynderickx for his help.

This work has been partially supported by Italian Space Agency (ASI) under the contract ARS 98/47.

References

S.A. Voronov et al., Geomag. and Aeron., Vol. 27, No. 3, p. 424, 1987.
A.M. Galper et al., NIM A248, p. 238, 1986.
L.V. Kurnosova et al., Kosmicheskie Issledovaniya, Vol. 79, No. 5, p. 711, 1991.
V.V. Akimov et al., 20^{th} ICRC, 2, p. 320, 1987.
S.A. Averin et al., Kosmicheskie Issledovaniya, Vol. 26, No. 2, p. 322, 1988.
A.M. Galper et al., *Radiation Belts: model and standards*, Geophys. Monogr., 1997.
U. Becker et al., 26^{th} ICRC, AIP Proceedings 516, edited by B.L. Dingus et al., p. 335, 2000.
J. Alcaraz et al., Phys. Lett. B, 484, p. 10, 2000.
S.A. Voronov et al., Cosmic Research, Vol. 33, No. 3, p. 329, 1995.
S.A. Voronov et al., Cosmic Research, Vol. 33, No. 5, p. 497, 1995.

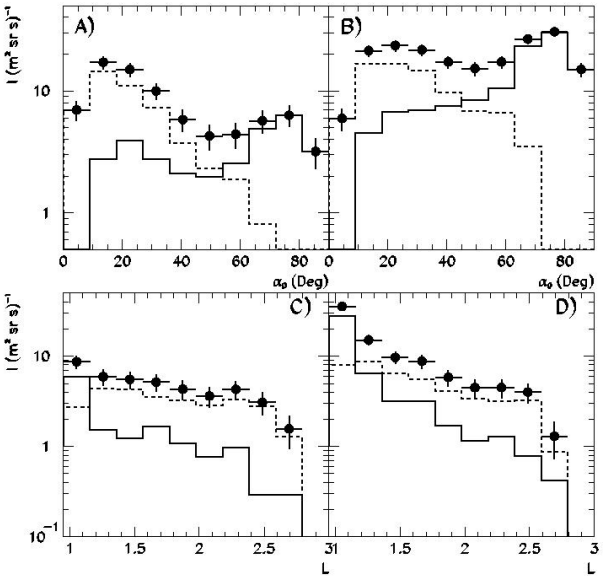

Fig. 7. Integral flux as function of α_0 and as function of L for e^- (A, C) and e^+ (B, D) between 0.205≤E≤2.73 GeV. The full line shows the long lived component, while the dashed one shows the short lived component.

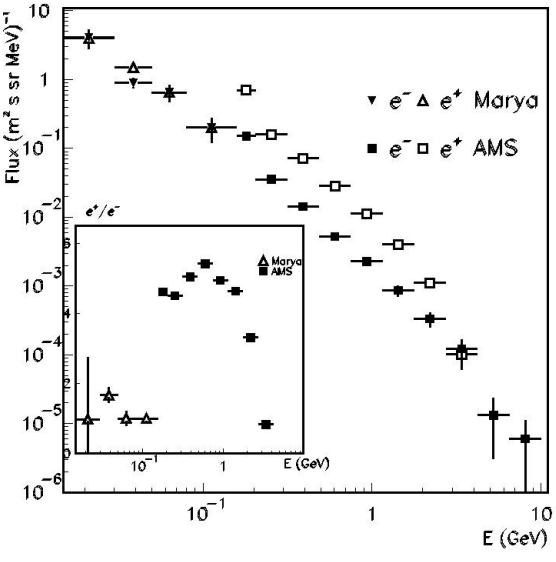

Fig. 8. Energy spectrum comparison between AMS and Marya for e^+ and e^- for particles with $\alpha_0 \geq 70^o$.
In the small plot the e^+/e^- ratio comparison is shown.